ICARUS 17, 346–372 (1972)

Variable Features on Mars: Preliminary Mariner 9 Television Results

CARL SAGAN, JOSEPH VEVERKA, PAUL FOX, AND RUSSELL DUBISCH

Laboratory for Planetary Studies, Cornell University, Ithaca, New York 14850

JOSHUA LEDERBERG, ELLIOTT LEVINTHAL, LYNN QUAM, AND ROBERT TUCKER

Department of Genetics, Stanford University Medical School and Artificial Intelligence Laboratory, Stanford University, Stanford, California 94305

JAMES B. POLLACK

Ames Research Center, Moffett Field, California 94035

AND

BRADFORD A. SMITH

Department of Astronomy, New Mexico State University, Las Cruces, New Mexico 88001

Received May 22, 1972

Systematic Mariner 9 photography of a range of Martian surface features, observed with all three photometric angles approximately invariant, reveals three general categories of albedo variations: (1) an essentially uniform contrast enhancement due to the dissipation of the dust storm; (2) the appearance of splotches, irregular dark markings at least partially related to topography; and (3) the development of both bright and dark linear streaks, generally emanating from craters. Some splotches and streaks vary on characteristic timescales ~2 weeks; they have characteristic dimensions of kilometers to tens of kilometers. The loci of these features appear in some cases to correspond well to the ground-based albedo markings, and the integrated time variation of splotches and streaks is suggested to produce the classical "seasonal" and secular albedo changes on Mars. The morphology and variability of streaks and splotches, and the resolution of at least one splotch into an extensive dune system, implicates windblown dust as the principal agent of Martian albedo differences and variability.

Introduction

That the bright and dark albedo markings of Mars are time variable has been known for more than a century. Contrast changes and, in many cases, attendant color variations, were reported by Schiaparelli, Lowell, Antoniadi, de Vaucouleurs, Focas, Dollfus, and many others. The color variations may be a psychophysiological phenomenon in which the eye/brain system attributes to a neutrally colored region adjacent to a brilliantly colored region a color complementary to the brilliant hue. Thus, while reports of color changes should not be taken at face value, some may, nevertheless, contain information on contrast changes. In addition to the wide range of visual reports, photographic (Slipher, 1962) and photometric (Focas, 1961) evidence of albedo changes exists. An impression of a progressive contrast change, proceeding in the spring hemisphere from the vaporizing cap toward and across the equator has been reported (see, e.g., Antoniadi, 1929; Focas, 1962) and has been given the name "wave of darkening" by de Vaucouleurs (1954). A statistical analysis (Pollack *et al.*, 1967) of Focas' data shows that, while some correlation exists between the season and the latitude of observed contrast enhance-

ments, the connection is far from one-to-one. Beside the seasonal changes, which are largely but not exclusively contrast enhancements between adjacent bright and dark areas, there are also a multitude of reports of secular changes (see, e.g., Antoniadi, 1929; Slipher, 1962), the nonperiodic and highly unpredictable variation in the boundaries between adjacent bright and dark markings—usually described in terms of the appearance or disappearance of a new albedo feature on the planet. The characteristic time scale for seasonal changes to develop (features several hundred kilometers across) is reported by ground-based observers to be several days (Dollfus, 1968).

Seasonal and secular variations on Mars have been attributed both in the scientific and in the popular literature for more than a century to the growth and decay of Martian vegetation, a conjecture impossible to disprove from the Earth or from Martian orbit because the hypothetical Martian organisms can have a wide range of conceivable attributes. An alternative detailed interpretation of these changes has been proposed (Sagan and Pollack, 1967, 1969; Sagan, Veverka, and Gierasch, 1971). The observed contrast variations are interpreted in terms of the alternate deposition and deflation of windblown dust having detectable contrast with respect to basement material. In this windblown dust model some seasonal effects are anticipated because the winds should be seasonally variable; and the relation of such changes to topography is to be expected, both because of winds induced by topography (Gierasch and Sagan, 1971) and because of topography acting as a sink or source of transportable material. Winds above the surface boundary layer required to move particles on the surface are calculated to be many tens of meters/second.

The Mariner 9 mission provides an ideal opportunity to examine Martian variable features. The resolution is improved by a factor of 100 to 1000, so that the mechanism of the changes may conceivably be revealed directly. The high resolution of the Mariner 9 observations permits us, for example, to test the hypothesis that a given change is due to the dissipation or formation of a long-lived obscuring cloud—a hypothesis extremely difficult to test with ground-based resolution. Moreover, ground-based restrictions on observable latitudes, longitudes, and seasons are to a considerable degree relaxed, because of the long operating lifetime of Mariner 9.

In the original conception of the two spacecraft Mariner '71 mission (see Masursky *et al.*, 1970), the orbit of one spacecraft was optimized for variable features investigations. To avoid misinterpreting brightness variations due to changing lighting conditions as intrinsic albedo changes, the spacecraft was to arrive over the same area of Mars with all three photometric angles close to constant every several days —the time scale for seasonal changes reported by ground-based observers. With the failure of Mariner 8 this strategy was necessarily abandoned, and Mariner 9 was placed into an orbit representing a compromise among various competing uses of the science systems. With the post trim orbital period just over 12 hr the Mariner 9 groundtrack drifts only about 9°/day. Accordingly the same region can be viewed on successive days with the illumination, viewing, and phase angles varying by $<10°$, a value quite acceptable for our purposes. We can, however, do much better by waiting 19 days. In that time, a particular groundtrack will have drifted halfway around Mars; the groundtrack of a zenith pass will be close to that of a nadir pass 19 days earlier, and vice versa. Such picture pairs can reproduce the lighting/viewing angles to 2–3°, and the phase angle to 5–10°. The control of the three photometric angles was decided upon because the extent of albedo variations, particularly at high resolution, was of course not previously known. Most of the albedo changes discovered were in fact so striking that they would have been observed even without careful control of photometric angles.

Through the end of the initial data taking on revolution 262, 27 variable feature target areas were systematically observed, as indicated in Fig. 1. These

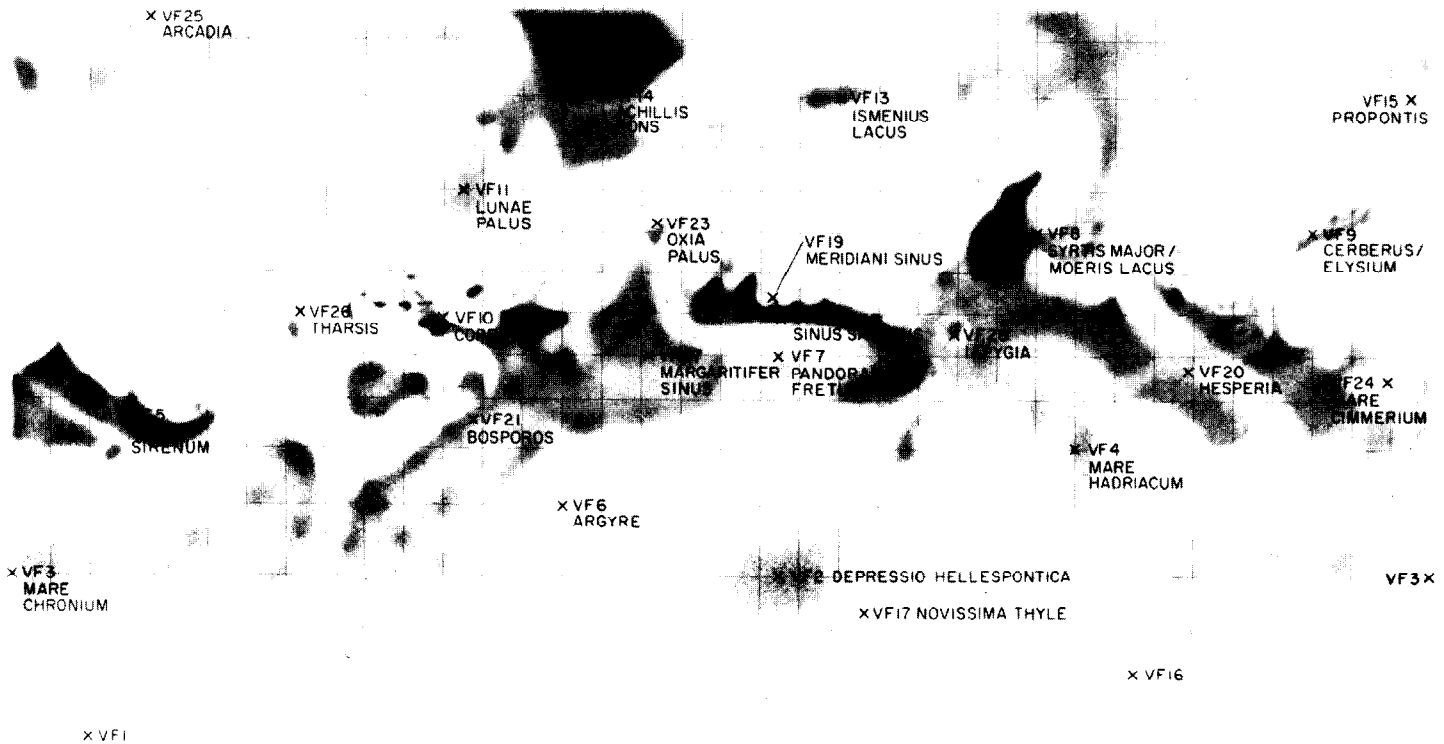

FIG. 1. Mercator map of Mars showing the locations of the Variable Features areas systematically observed during the Mariner 9 mission. Two areas, VF1 at (75°S, 160°W) and VF16 at (70°S, 254°W) fall outside the map boundaries, and their indicated positions are schematic.

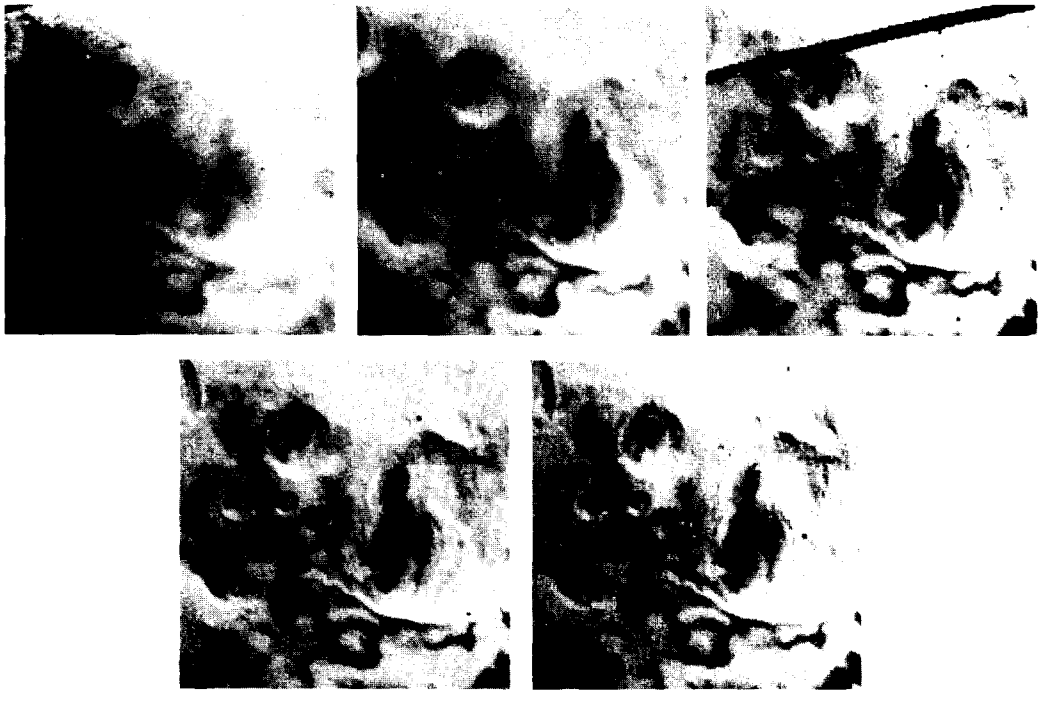

FIG 2. Five views of the same region in Thyles Mons (75°S, 160°W) as it appeared on revolutions 18, 78, 113, 152, and 191 (top left to bottom right). These are sections taken out of Mariner 9 wide angle A frames. Approximate width = 290km. (STN 0163:040909, 10, 11, 12).

areas represent a wide range of albedos, positions, topographies, and elevations. They include regions reported in the classical literature to be highly time variable and regions reported to be quite stable. Until the failure of the filter wheel on revolution 118, some of these regions were observed in three colors and in three polarizations, with the polarization vector stepped in 60° increments. After revolution 118 all A-camera observations were made with an effectively orange polarization filter. All high resolution B-frame photographs have been obtained with a yellow filter. In addition to areas specifically designated as variable features targets, overlapping mapping frames provide an important additional source of variable features information, with turnaround times of 19 days.

In the time interval between the decay of the dust storm and the end of the nominal mission on revolution 262 a very wide array of surface albedo variations have been discovered. The systematic character of these changes, particularly in cases where there are many successive observations and changes observed over only a small fraction of the frame, clearly show that the observations reported here are not due to any progressive photometric deterioration of the camera systems. Other, especially atmospheric, variations are reported elsewhere (Leovy *et al.*, 1972). All photographs which accompany this article have been contrast enhanced by computer processing.

DISSIPATION OF ATMOSPHERIC DUST

At least three general categories of albedo variations were discovered by Mariner 9: (1) an essentially uniform contrast enhancement with time over broad regions, coinciding with the decay of the dust storm; (2) the appearance of irregular dark markings which we here call splotches; and (3) the development of

variable linear features to be described below which are called streaks or tails. An example of category 1 changes is shown in Fig. 2, a sequence of photographs of the Thyles Mons region at (75°S, 160°W). The progressive nature of the contrast enhancement, and the correlation of these changes with the time scale of dust settling as determined by a variety of techniques (Masursky *et al.*, 1972; Hord *et al.*, 1972; Hanel *et al.*, 1972; Neugebauer *et al.*, 1972) clearly indicate such changes to be a consequence of the dissipation of the great dust storm. A characteristic settling time scale of weeks implies particle sizes $\geqslant$ some tens of microns (Pollack and Sagan, 1969; see also Leovy *et al.*, 1972). In addition, there is a range of cases which are clearly due to the drifting of a small cloud over an area with attendant obscuration and subsequent improvement of the detectivity of surface features (see, e.g., Leovy *et al.*, 1972). Leovy *et al.* exhibit a dust storm which left the underlying area darkened in its wake with a characteristic time for albedo change of $\leqslant$19 days, which they point out is consistent with the windblown dust model (Sagan and Pollack, 1967, 1969). The array of parallel curvilinear streaks extending 1000km southwestward from South Spot, as observed in the early phases of the Mariner 9 mission (Masursky *et al.*, 1972), also proved to be time variable.

At least some areas of Mars are predicted to have long-lived and recurrent dust palls above them related to the topography (Sagan, Veverka, and Gierasch, 1971). produced by, for example, slope and obstacle winds, and it is conceivable that

FIG. 3. Section of A frame showing the region of Depressio Hellespontica (60°S, 345°W) on revolution 153. Approximate width = 120km. (IPL 490:134154).

some small-scale changes reported below may be due to the long-term presence followed by the rapid dissipation of such a localized cloud. However, such processes appear to us meteorologically implausible, particularly in cases where the hypothetical cloud must be absolutely stationary for periods of weeks or months and then dissipate rapidly. In most cases the distinction between changes induced by the dissipation or motion of overlying clouds and changes in the actual surface material is apparent: In the former case, both the distribution of albedo and visible topographic detail vary, and topographic features are not well-defined; in the latter case, the topography is well-defined and only the albedo distribution varies.

Splotches

Many of the classical dark areas of Mars are revealed, when viewed with Mariner 9 resolution, to have a mottled appearance. For example, Depressio Hellespontica is resolved into a bright cratered terrain generously sprinkled with dark irregular splotches (Fig. 3). Splotches have characteristic dimensions between several kilometers and several tens of kilometers. They often appear to lie within craters and sometimes seem to wash over crater walls. Splotches seem to be controlled by topography since they are common near the inside and outside of crater walls and along what appear to be ridges or scarps. The true contrast of a typical splotch with respect to its surroundings is some 10 or 15%. The larger splotches and splotch complexes are several hundred kilometers in lateral dimensions. These two facts imply that the largest splotches should be visible under ideal seeing conditions by observers on Earth. It is notable that observers such as Focas (1961) have reported the Martian dark areas to be composed of irregular detail which Focas called "dark nuclei."

A preliminary comparison of Mariner 6 and 7 topography of Mars, obtained in 1969, with Mariner 9 photography of Mars in the same regions, obtained in 1971/1972, indicates the appearance and development of splotches in this time interval. We have found many cases of large scale development of splotches in time scales between several months and <2 weeks. We have found no clear cases of the development of splotches on a time scale of 1 day. Thus, the characteristic dimensions, contrasts, and variational time scales of splotches are consistent with the observations of Focas. We have not yet sought agreement between the positions of the dark nuclei of Focas and of the large splotch complexes uncovered by Mariner 9.

Data from different orbits have been processed, in a search for variations, at the Artificial Intelligence Laboratory of Stanford University. In an interactive procedure described by Levinthal *et al.* (1973), the regions common to the two pictures are isolated, calibrated, scaled, rectified, and then differenced, picture

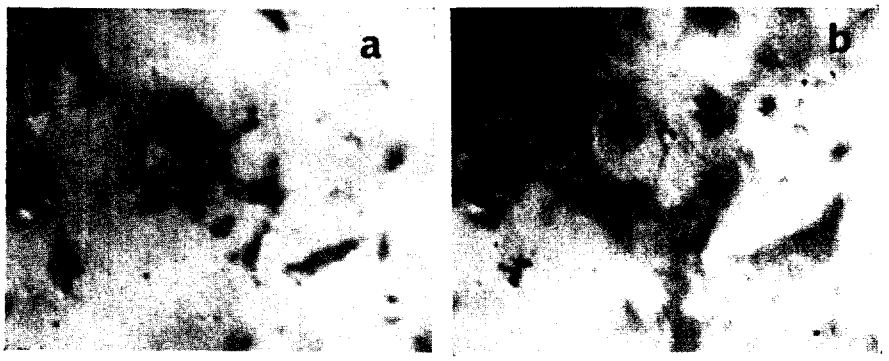

Fig. 4. Two views of Depression Hellespontia (55°S, 345°W). Left: revolution 153. Right: revolution 227. Shown are sections of A frames. Approximate width = 360 km. (STN 0163: 040906).

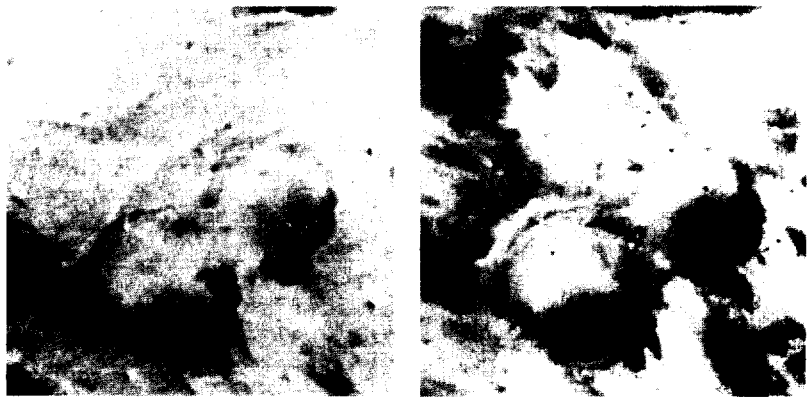

FIG. 5. Two views of Pandorae Fretum (25°S, 335°W). Left: revolution 108. Right: revolution 188. Shown are sections of A frames. Approximate width = 160km. (STN 0162:04109).

element by picture element. The differenced pictures should be featureless in cases where no changes have occurred, but should strikingly display regions of variation where they occur. Figure 4 displays a region in Depressio Hellespontica, near (55°S, 345°W), as it appeared on revolution 153 (at left) and revolution 227 (at right). Much of the intercrater area has darkened considerably and some splotches within craters have changed. The area involved in the change is approximately 400 × 600km. A biological interpretation of this variation implies that a major bloom of organisms occurs in 38 days over an enormous area. On the windblown dust model fine dust has been deposited over the entire area and was subsequently scoured off by strong winds. As in many other cases presented below, the biological explanation cannot be excluded, but the windblown dust explanation appears to be a more natural interpretation of the observed variable features.

Figure 5 exhibits changes in splotches in and around two craters in Pandorae Fretum, a seasonal and secular variable in the classical literature. The larger crater is about 60km across; the time interval between the two views is 38 days. Such variations of crater-connected splotches are typical in our data. In Fig. 6 is an example of another typical change observed in splotch areas—the development of dark areas along topographic features such as ridges and crater walls. The region

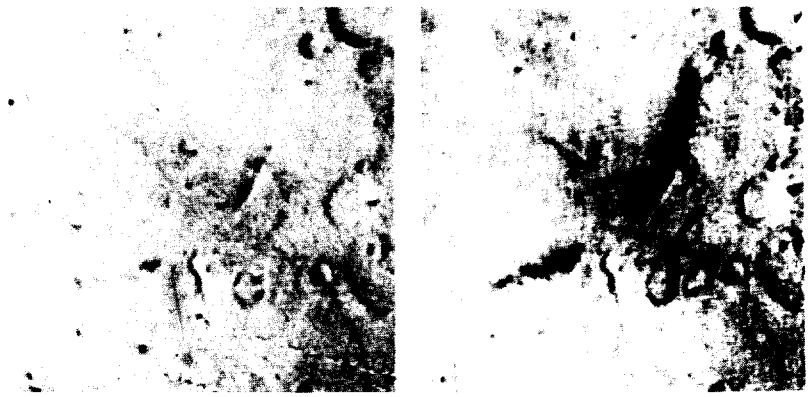

FIG. 6. Comparison of A-frame sections showing a region of Pyrrhae Regio (25°S, 15°W). Left: revolution 137. Right: revolution 176. Approximate width = 130km. (STN 0160:030406).

is Pyrrhae Regio. Sections of A-frames are shown; the linear dimension is about 125km, and the time interval between the two views is 19 days. In this case, dark material has appeared against an arcuate topographic feature which may be the remnant of an ancient crater wall. In addition, dark material has also appeared along the rim of the smaller crater below. Hypothetical Martian vegetation might grow preferentially along topographic features—for example, to insure stabilization against winds. In the windblown dust model, we are observing either the deposition of dark material by winds blowing generally at right angles to the ridges or the scouring of bright fines by winds blowing along the ridges (cf. Bagnold, 1960, pp. 142–3).

In addition to splotch variations at A-frame resolution shown in the last three figures, we have also uncovered cases of very major changes at B-frame resolution. Figure 7 displays a low-resolution view of the region between Thyles Collis and Depressio Magna at about (70°S, 259°W). The splotches of interest are those indicated near the center of the frame between the two craters. Figure 8 shows a high resolution photograph of this intrinsically

FIG. 7. Wide-angle (A-camera) view of the region between Thyles Collis and Depressio Magna near (70°S, 259°W) on revolution 179. The arrow indicates the area of the next figure. Approximate width = (IPL 1283:220256).

FIG. 8. High-resolution (B-camera) view of the area outlined in Fig. 7 at about (70°S, 254°W). Note especially the dark leaf-shaped area just below the crater. Revolution 179. Approximate width = 75km. (IPL 359:080348).

high-contrast region. We note especially the scalloped boundary between bright and dark materials, which is strongly suggestive of aeolian transport, a point to which we return later. On the basis of this photograph, however, it is difficult to decide whether it is bright or dark material which is being blown. Figure 9 is a comparison of the center of the region shown in Fig. 8 on revolution 99 and on revolution 122. In this period of 13 days an entire albedo marking, shaped like a spearhead or a leaf, suddenly appeared. In addition to the appearance of the leaf-shaped appendage on its stem, the boundary of one of the dark areas at left moved to the right. In a period of <13 days a 10-km dark area has appeared discontinuously and remained essentially unchanged in appearance for many months thereafter, a variation suggestive of saturation phenomena. In biological models, the surface goes from no or sparse cover of organisms to saturation surface density in ~1 week. On the windblown dust model, most of the transportable material which can be removed or deposited is removed or deposited in ~1 week, in the case of removal exposing the underlying material of contrasting albedo. The observations can be understood with either bright or dark transportable material.

An apparently typical dark splotch area is seen in Fig. 10, an A frame. However, a high-resolution B frame (Fig. 11) of the dark splotch within the crater at bottom right in Fig. 10 reveals that the dark splotch is a dune field. It is certainly not true that all dark splotches are dune fields, but this example proves that dark

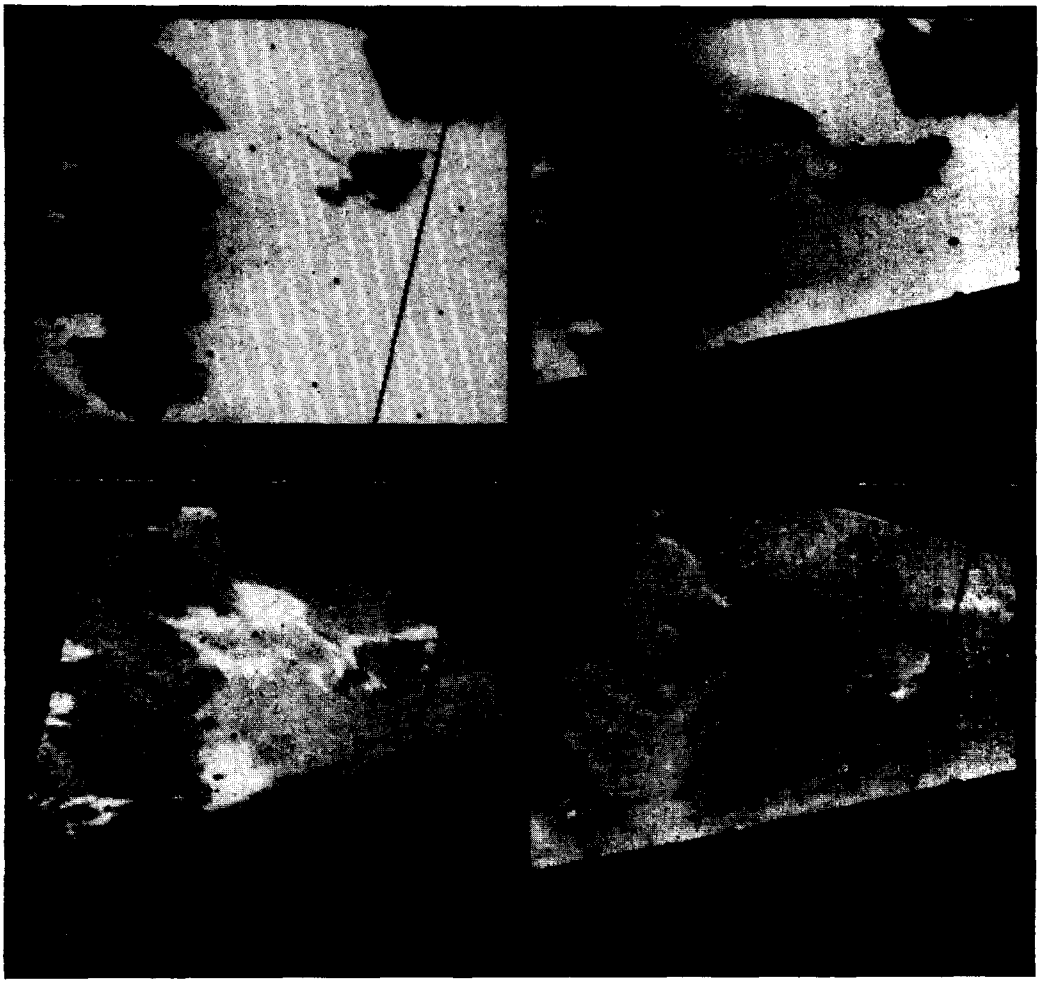

FIG. 9. Comparison of the appearance of the central area of Fig. 8 on revolution 99 (top left) and on revolution 126 (top right). After the two views were similarly scaled and projected, the view at top right was aligned and registered to that at top left, picture element by picture element. Then the two views were differenced, again picture element by picture element. Shown at bottom left is the 99–126 difference; at bottom right, the 126–99 (reverse) difference. Approximate width = 45km. (STN 0153:012201).

FIG. 10. Wide-angle (A-camera) view of a splotch field in Hellespontus near (45°S, 330°W) on revolution 112. Note especially the large splotch inside the crater at lower right. Approximate width = 430km. (IPL 1863:112847).

FIG. 11. High-resolution (B-camera) view of the dark splotch referred to in the previous figure, revealing a dune field near (48°S, 330°W). Revolution 229. Approximate width = 65km. (MTVS 4264:16).

material is efficiently moved by Martian winds. Sand dunes on Mars were suggested by Gifford (1964), and further discussed by Belcher *et al.* (1971).

STREAKS

While some classical variable features on Mars are resolved into splotchy terrains as indicated above, other are revealed by Mariner 9 to be composed of a new category of Martian albedo features not reported by classical observers, arrays of streaks. Figure 12 shows one such region, Hesperia, the sometime dusky or semitone region between Mare Tyrrhenum and Mare Cimmerium which seems to be made up of bright streaks associated with craters.

A credible explanation of such arrays of long parallel streaks emanating from craters is that fine bright dust, transported into the craters in the waning stages of the dust storm (see below) was subsequently blown out by high velocity winds having a prevailing direction. In this view, the streaks are downwind of the craters. The length and half-angle of the streak may be some measure of the velocity of the wind which deflated the crater. If this conjecture is corroborated, there are natural wind direction indicators and conceivably anemometers laid out on the Martian surface.

Bosporus, a darkish area near Solis Lacus, is resolved into a host of dark cometlike tails or streaks, again associated with craters and again reflecting a predominant direction (Fig. 13). Some of these dark streaks are more than 50km long, yet remain very narrow (~5km) throughout their length. They are too small

FIG. 12. A-camera view of a region in Hesperia (23°S, 242°W). Resolution 128. Approximate width = 400km. (MTVS 4155:84).

FIG. 13. A-camera view of a region in Bosporus (34°S, 62°W). Revolution 129. Approximate width = 400km. (MTVS 4156:72).

to be individually resolved by ground-based observers. A comparison of Figs. 12 and 13 indicates that dark streaks tend to have a larger half-angle than do bright streaks, although a class of very long dark narrow streaks also exists. Three explanations of dark streaks suggest themselves. The first possibility is that dark streaks represent the wind shadows of crater ramparts and that the dark streaks can be understood in terms of bright material deposited by a dust storm on underlying dark material everywhere but downwind of craters. This explanation seems to us unlikely, because of cases where new dark tails have developed while the relative contrasts between older dark tails and their surroundings remain unaltered. The second possibility is that dark material is deflated downwind from the crater bottom. The third possibility is that turbulence downwind of the crater scours bright fines preferentially in that area, although we have no understanding of the dynamics of such a process. Mixed classes of streaks exist. Figure 14, for example, shows a set of bright streaks with dark borders in Syrtis Major.

Syrtis Major exhibits a very large surface density of streaks, bright, dark, and mixed. Some dark streaks are irregular and morphologically quite different from those occurring anywhere else on the planet (Fig. 15). Because of the very steep slopes on Syrtis Major, higher winds may be more frequent there than in most other surface regions of the planet (Gierasch and Sagan, 1971). It has been proposed that two different varieties of winds occur in Syrtis Major, one blowing along

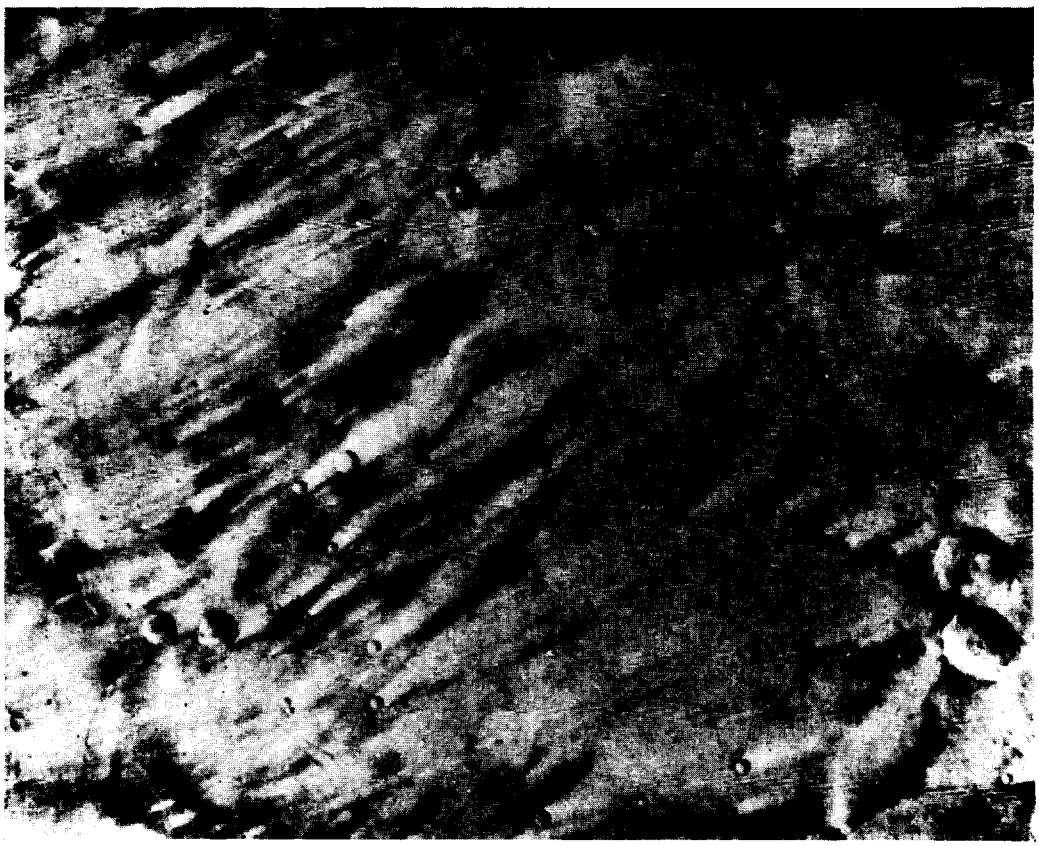

FIG. 14. A-camera view of a region in Syrtis Major (4°N, 295°W). Revolution 153. Approximate width = 500 km. (IPL 490:184752).

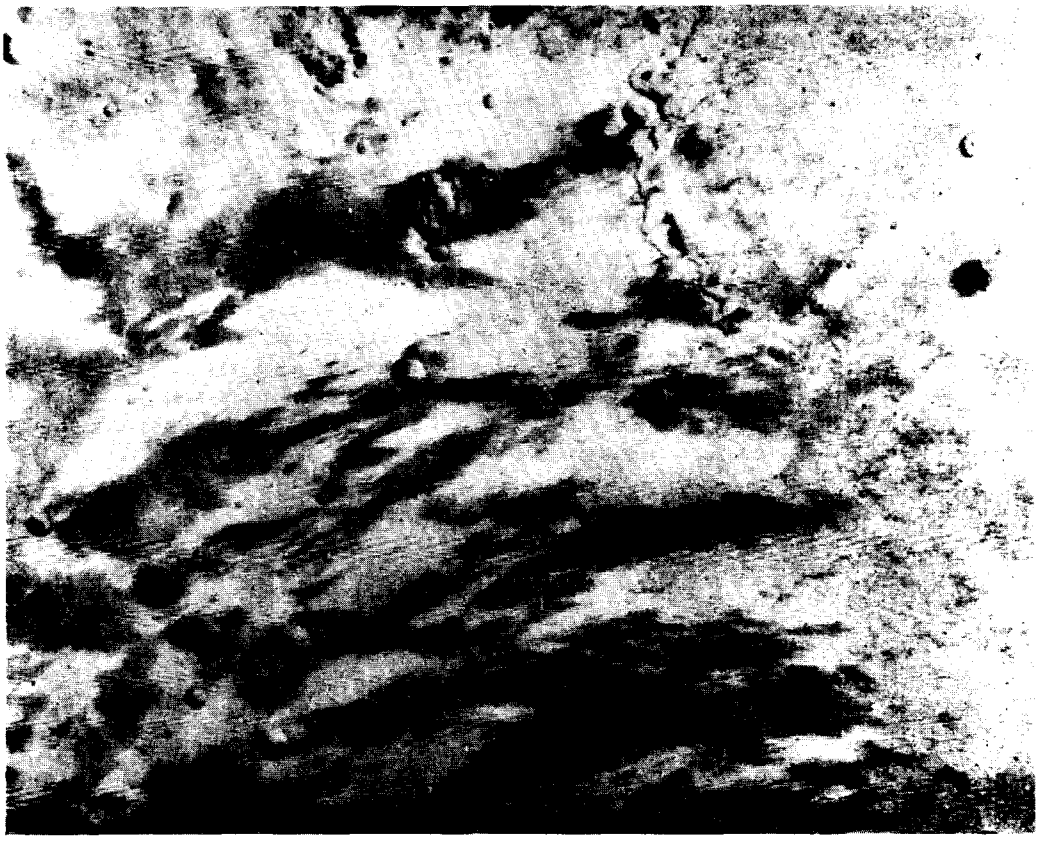

FIG. 15. A-camera view of another portion of Syrtis Major (13°N, 283°W). Revolution 155. Approximate width = 540 km. (IPL 488:100143).

the slope, the other blowing across the slope (Sagan *et al.*, 1971). Such strong crosswinds could conceivably produce the irregular streaks observed.

In Fig. 16 are plotted all apparent bright, dark and mixed albedo streaks in Syrtis Major, superposed on a map showing the classical boundaries of Syrtis Major. It is apparent that the loci of streaks correspond rather closely to the configuration of Syrtis Major as seen from Earth.

The evident aeolian origin of the streaks immediately suggests that the classical seasonal and secular albedo variations reported for such areas as Syrtis Major are due to the production and dissipation of bright and dark streaks. We have observed many cases of variations in dark streaks during the course of the mission. Figure 17 is a comparison of streaks within Syrtis Major in revolutions 155 and 233. The configuration of irregular dark streaks is clearly variable on a time scale of 38 days. According to Antoniadi (1929) it is the eastern flanks of Syrtis Major which exhibit the greatest seasonal variations (Fig. 18). It is notable (Fig. 16) that this flank is a region of high-density dark variable streaks.

In Fig. 19 are shown two views of the Daedalia region near Solis Lacus. The first, obtained on revolution 115, shows a cratered terrain with very few dark streaks. By revolution 195, shown on the right-hand side of Fig. 19, the area had darkened considerably due to the appearance of numerous dark wide-angle streaks behind most of the craters. Figure 20 shows a closeup view of an individual crater in this area behind which a dark tail about 50 km long appeared in 38 days.

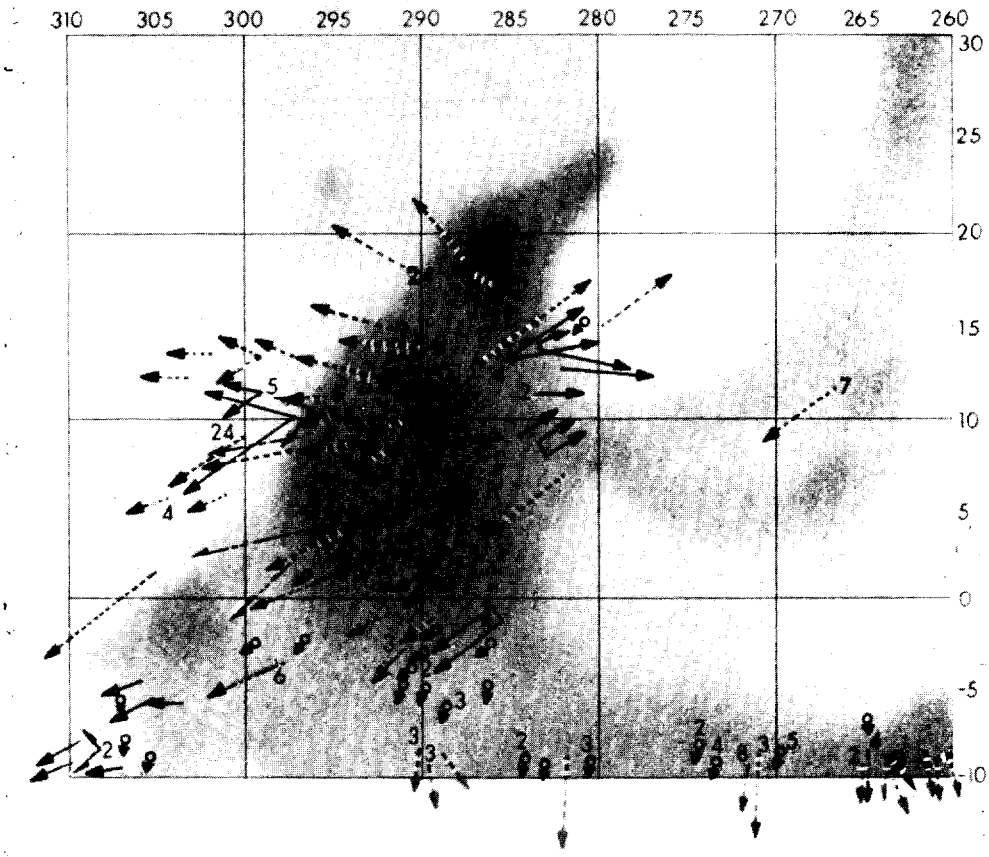

FIG. 16. Streak map of Syrtis Major. The full arrows represent dark streaks, dashed arrows bright streaks, and dash-dotted arrows bright streaks with dark borders (cf. Fig. 14). Circles with short arrowheads represent craters with rudimentary streaks. Whenever numerous streaks of one type occur in a small area, only one streak is shown, along with the number of such streaks in the area. The streak length is exaggerated by a factor five.

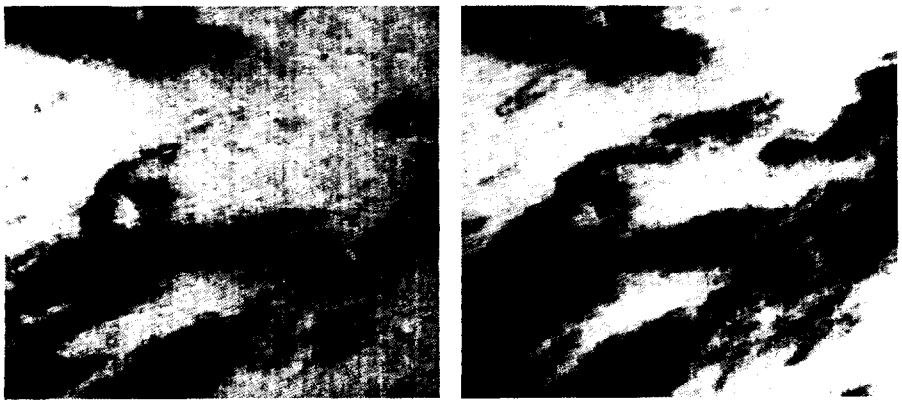

FIG. 17. Two views of a streaked area within Syrtis Major (15°N, 28°W). On the left: revolution 155. Right: revolution 233. Shown are section of A frames. Approximate width = 140km (STN 0164: 041505).

FIG. 18. Antoniadi's map summarizing classically reported seasonal changes in Syrtis Major. Note that the eastern boundary is variable, while the western appears to remain stable. Unlike all other photographs in this article, South is here at the top.

FIG. 19. Two views of a region in Daedalia (25°S, 125°W). Left: revolution 115. Right: revolution 195. Shown are sections of A frames. Approximate width = 340km. (STN 0162: 040105).

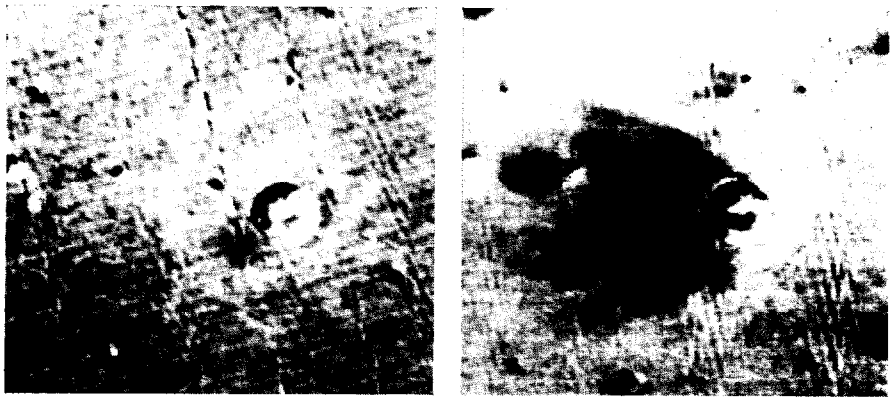

FIG. 20. Two views of a crater near the center of Fig. 19. Again on the left: revolution 115; on the right: revolution 195. Shown are sections of A frames. Approximate width = 100km. (STN 0162: 040107).

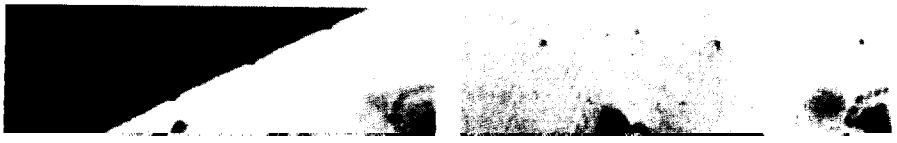

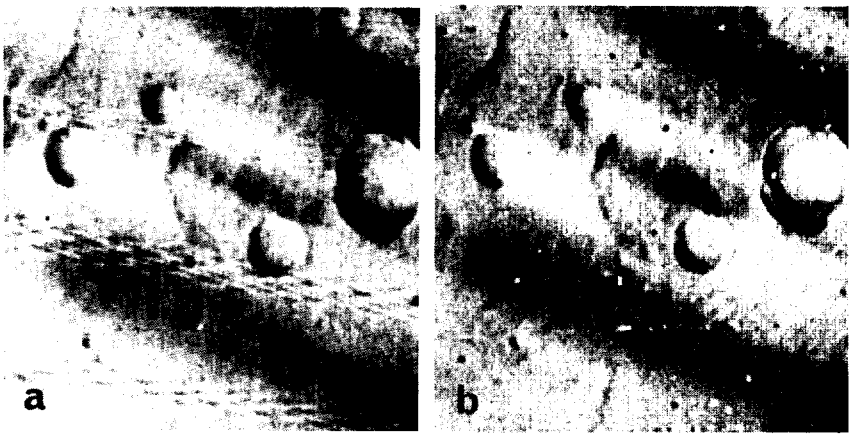

FIG. 22. Two views of a region in Hesperia (25°S, 245°W) showing the stability of bright tails. Left: revolution 128. Right: revolution 167. Shown are sections of A frames. Approximate width = 90km. (STN 0160:030409).

A similar case is the comparison in Fig. 21 of a region in Mare Erythraeum at the left on revolution 133 and at the right on revolution 211. A new dark tail as well as several other dark regions have developed in this time interval.

Ground-based observations of Mars, made at New Mexico State University Observatory, showed that Hesperia was dark and indistinguishable from the adjacent maria Tyrrenum and Cimmerium in September 1971, before the dust storm. But Hesperia was noted to be appreciably brighter when the dust cleared in January 1972. The brightening of Hesperia took place during the dust storm, when the surface of Mars was hidden from view. The Mariner 9 high resolution appearance of Hesperia (Fig. 12) suggests that this brightening is due to the generation of numerous bright streaks, or possibly the removal of previously coexisting dark streaks.

Our observations show the white streaks to be very stable. Figure 22 shows little or no variation in the bright streak configurations in Hesperia over a period of 38 days. Later, however, in a time interval of 19 days (Fig. 23) crater-associated dark streaks developed, while in the same interval no variation whatever is evident in the bright streaks. These changes illustrate the general trend for bright tails to be much more stable than dark tails. While we have circumstantial evidence, from ground-based observations mentioned above, for the development of new bright

FIG. 23: Two views of a region in Hesperia (25°S, 245°W) showing the stability of white tails and the appearance of dark tails. Left: revolution 128. Right: revolution 206. Shown are sections of A-frames. Approximate width = 220km. (STN 0164:041501).

tails, we have so far failed to notice any new bright tails appearing or existing bright tails changing anywhere on Mars during the course of the mission. On the other hand, numerous changes in dark streaks on a time scale $\leqslant$19 days have been uncovered. The general trend since the termination of the dust storm has been for more dark streaks to appear and for existing dark streaks to increase in size. The net effect is that dark areas have increased at the expense of adjacent bright areas. Such a trend cannot continue indefinitely, and it may be that by Earth summer of 1972, Mariner 9 will observe a statistical reversal of this trend.

The development of dark streaks in Hesperia (Fig. 23) by a process which produces no discernible changes in the bright streaks emanating from the same craters is extremely interesting and implies that the process which produces dark streaks requires lower wind velocities than the process which alters bright streaks, at least in this area.

Figure 24, an A-frame view of an area in Tharsis, is characterized by a wide assortment of bright streaks. No variations in the configuration of these streaks have been observed through late in the mission. Figure 25 shows, in high resolution, the complex structure of part of the wedge-shaped bright streak complex near right center of Fig. 24. The straightness of these streaks, the longest of which extends for 50km, the precision with which they join each other, not transgressing to the opposite side of the transverse streak,

FIG. 24. A-frame view of a region in Tharsis (10°S, 107°W). Revolution 156. Approximate width = 410km. (IPL 1108:150842).

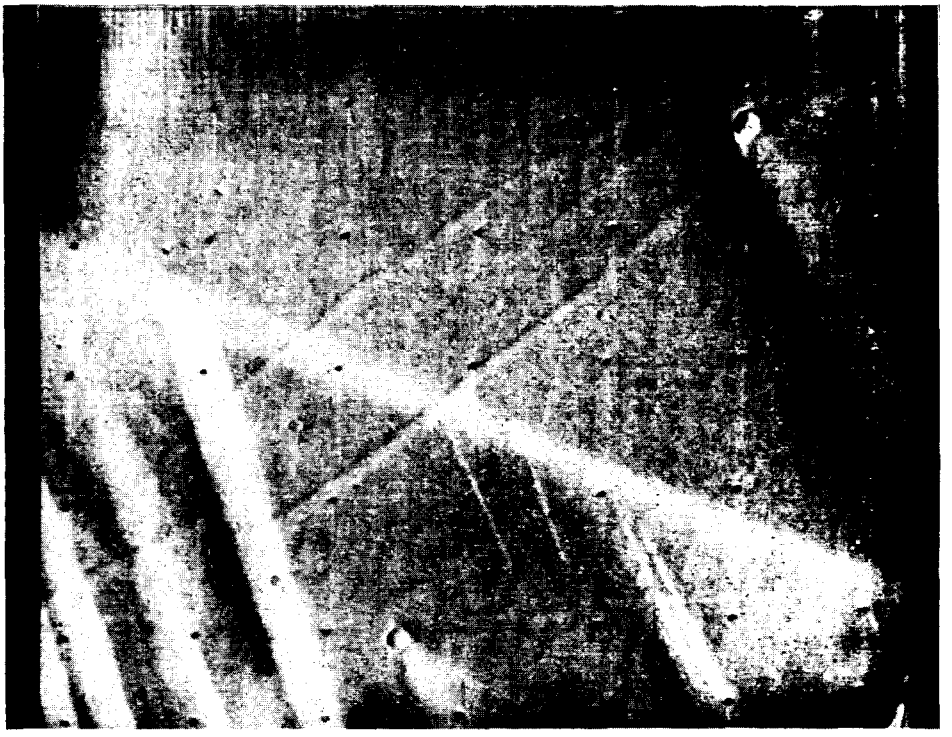

FIG. 25. High-resolution (B-camera) view of a complex streak pattern near the center of Fig. 24, at (11°0S, 105°4W). Revolution 236. Approximate width = 45km. (MTVS 4271:31).

FIG. 26. High-resolution (B-camera) view of a group of bright streaks near the left-center of Fig. 24, at (9°5S, 108°4W). Revolution 234. Approximate width = 45km. (MTVS 4269:46).

and their time invariability together pose an interesting problem. There is a definite suggestion here, as elsewhere, of information which will lead to an aeolian depositional stratigraphy, since it is improbable that all the streaks in Fig. 25 were formed simultaneously. Figure 26 displays a high-resolution view of the area near left center of Fig. 24 where a bright transverse streak crosses what appears to be faults in the vicinity of many other bright streaks. The origin of the streaks in an evident topographic feature is reminiscent of other cases of topographic control (e.g., Figs. 5 and 6) and suggests that topographic irregularities other than craters may be repositories of fine material which later is wind-transported from these topographic features.

Some of the dark tails in Bosporus (Fig. 13) or in Daedelia (Fig. 19) may be deflationary in character; that is, resulting from scouring of fines downstream of craters or other topographic irregularities. However, other dark streaks, such as those shown in Fig. 27, may be depositional in character. This is an A frame of a region in Cereberus near Elysium. The upper crater, about 30km across, can be interpreted as the source of dark material carried downwind to produce the intense dark tail. In the process, part of the rim of the smaller crater appears to have been covered by dark material. Note a shadow zone behind the smaller crater where no dark material was deposited. This is another case from which aeolian depositional stratigraphic relationships are expected to emerge. We know of no other dark streak so similar in shape to bright streaks.

Discussion

A variety of classical time-variable bright and dark areas on Mars are found to be constituted of, and have their variations controlled by, the distribution

Fig. 27: Wide-angle A-frame of a region in Cerberus, near (9°N, 191°W). Revolution 179. Approximate height = 435km. (MTVS 4207:89).

and appearance of two categories of features: splotches and streaks. There are apparently only dark splotches, but both bright and dark streaks. Both are connected with topography, particularly craters, ridges, scarps, and faults. Some cases, possibly intermediate between streaks and splotches, also exist, and it may be that the essential distinction between the two types of features has to do with wind velocity. The parallel arrangement and streamlined shape of the streaks points very strongly to an aeolian origin. A given variation in a streak or splotch requires the deposition or removal of only a thin layer of material, easily sequestered in craters or elsewhere.

The serrated interface between bright and dark areas in some splotches (see, e.g., Fig. 8) is also very reminiscent of aeolian transport. When a longitudinal pile of rock flour of particle size in the 100μ range characteristic of the Martian surface (Pollack and Sagan, 1969; Neugebauer *et al.*, 1971) is exposed to not atypical (Sagan *et al.*, 1971) Martian wind velocities $\sim$100 m/sec, a pattern like that in Fig. 8 is formed (Hertzler, 1966a). While the homology transformation must scale over a factor of 10^5, the wind tunnel results are provocative and support the aeolian origin of splotches. The resolution (Fig. 11) of some dark splotches into dune fields demonstrates the aeolian character of at least some splotches.

The bright streaks are most readily understood if we assume that, in the waning stages of the dust storm, fine particles, settling through the atmosphere, are preferentially trapped in topographic features such as craters by lateral transport. Deflation of craters by subsequent high-

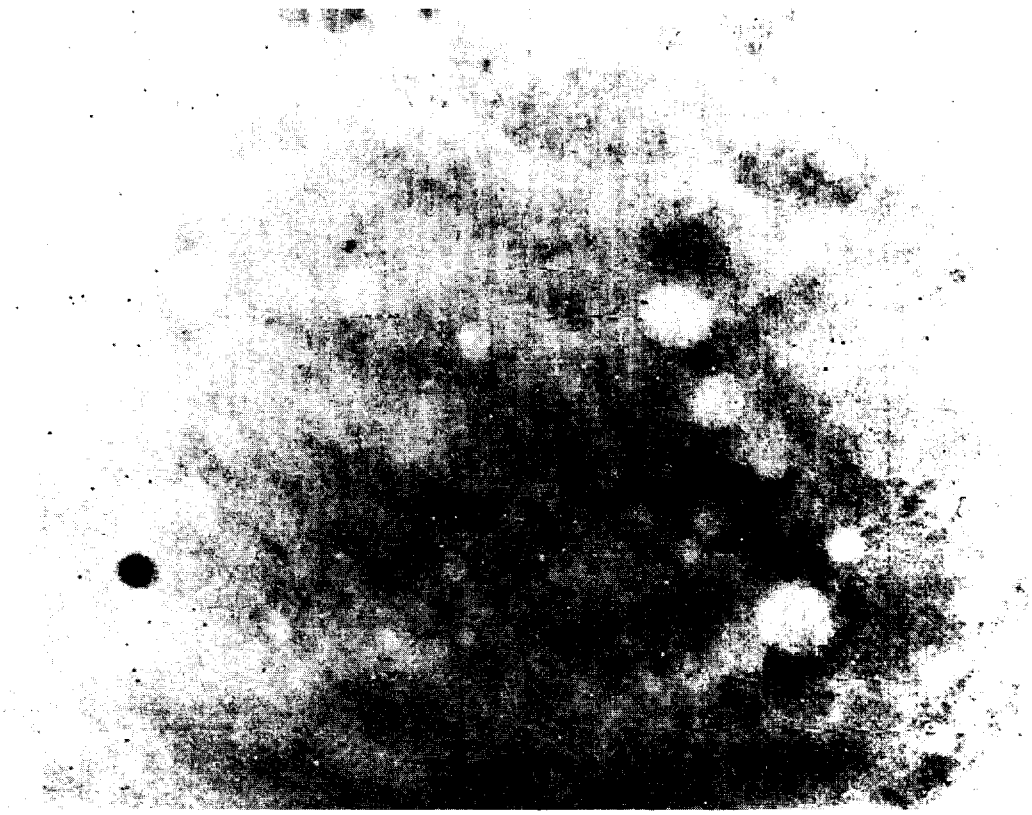

FIG. 28. A portion of a global A frame taken during the waning stages of the 1971 dust storm showing numerous bright craters. The dark spot at lower left is a camera defect. Revolution 44. Frame center (35°S, 29°W). Approximate width = 200 km. (IPL 930:222549).

velocity winds produces the parallel array of streaks. The appearance of bright craters towards the end of the dust storm (Fig. 28) is consistent with this idea, although some contribution to higher albedo follows from the longer slant path through a dusty atmosphere above craters than above neighboring terrain.

Thus, while an excellent case can, in our opinion, be made for the aeolian origin of both splotches and streaks, there are many detailed questions which remain unanswered: Is a given dark splotch or streak due to the deflation of overlying bright material or the deposition of dark material? If the latter, what is the source of the dark material? Why do some dark streaks have an appearance as in Fig. 13, while others (Fig. 27) resemble closely the form of bright streaks? Is a given topography-related dark region due to the preferential removal of overlying bright material downwind of the obstacle or to the wind shadowing of downstream areas upon deposition of bright material on the surroundings? In serrated interfaces between bright and dark material (cf. Fig. 8), which boundary of the dark splotch (dendritic protrusions or amorphous edge) is in motion? Many of these questions will be approached in work now underway—in a wide range of statistical studies, in the pursuit of stratigraphic relations, and in frames where several wind indicators, among them serrated edges, streaks, and splotches, are simultaneously present.

While detailed statistical studies are now in progress, preliminary results indicate no progressive latitudinal dependence of the observed albedo changes. If this is typical on Mars, and not a consequence of conditions following a major dust storm, then the phrase "wave of darkening" is a misnomer. Nevertheless, there is a real time-dependence of albedo changes, which were much more apparent all over Mars after revolution 200 than at any other time during the mission.

The evidence presented above suggests the transport of both bright and dark material on Mars. Yet the transport of bright material must, in the long term, dominate. In a plot of mean particle radius versus threshold velocity for initiating particle motion within the surface velocity boundary layer (or, equivalently as displayed in Fig. 29, the corresponding velocity above the boundary layer), there exists a minimum in the curve corresponding to a most easily transported particle size. Larger particles are more immobile because the lift varies with the square of the particle dimensions while the mass varies with the cube. Smaller particles are more immobile because they are unaffected by the turbulent eddies producing the motion. For Martian conditions the most readily transportable particles are in the 200μ range (Sagan and Pollack, 1967, 1969). However, such particles saltating along the surface exchange momentum with the surface and splay out smaller suspendable particles, not easily lifted by the winds directly. The net result is the preferential injection into the atmosphere of small particles which fall out slowly according to the Stokes–Cunningham equation or even more slowly if turbulent support exists. For single composition models, the smaller particles are (because of multiple scattering) expected to be brighter than the larger particles. Dark tails developed in Hesperia by processes which did not affect the preexisting bright tails (Fig. 23). In the filling of craters by dust fallout, the smallest particles arrive last. These particles, deflated by poststorm high-velocity winds,

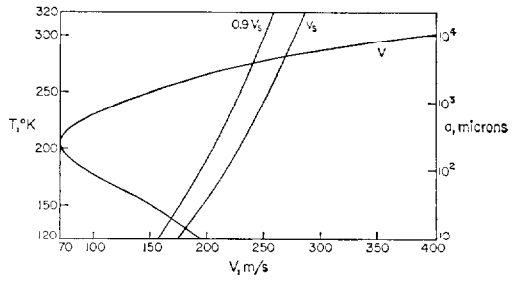

FIG. 29. The curve labeled V shows the velocity above the surface boundary layer required to move particles of radius a on the Martian surface. (After Sagan and Pollack, 1967.) Also shown is the temperature dependence of the velocity of sound V_s, and of 0.9 V_s.

would be difficult to move once layed down in bright streaks (Fig. 29). But deflation of larger dark crater particles, nearer to 200μ radius, could still be accomplished by winds of lower velocity which leave the bright streak particles unmoved.

However, single composition models, while they provide a convenient starting point, are geologically oversimplified. It may be (Sagan *et al.*, 1971) that, because of the greater area to volume ratios of small particles and the presence of oxidizing compounds such as ozone in the Martian atmosphere, there is a statistical connection between particle size and composition. The smaller particles would be more oxidized. The Mariner 9 IRIS results (Hanel *et al.*, 1972) suggest a variety of siliceous minerals on the Martian surface, and the existence of major summit calderas indicates in another way that the planet has been differentiated (McCauley *et al.*, 1972). It is possible that the bright and dark material corresponds to different atmospheric exposure ages of basaltic or other minerals. As long as the planet remains geologically active we would no more expect a complete homogenization of such components on Mars than we do on the Earth. This view evokes in several ways the "volcanic–aeolian" hypothesis of Martian albedo features (McLaughlin, 1955), which now appears remarkably prescient in at least some of its features. An additional possibility is that all wind-blown constituents may not have the same density. Small particles of volcanic tuff with a large empty fractional volume or nonspherical particles such as mica flakes may be much more readily transportable than solid or spherical particles of the same dimensions. In a given aeolian transport event, we expect both saltation of coarse particles and suspension of fines.

Wind velocities ~100 m/sec are deduced from lee wave clouds (Leovy *et al.*, 1972) and from the IRIS atmospheric temperature structure via the thermal wind equation (Hanel *et al.*, 1972), as well as from a variety of theoretically expected wind regimes (Sagan *et al.*, 1971), lending some support to the calculations exhibited in Fig. 29. Such high-velocity sandblasting in the thin Martian atmosphere should result in aeolian erosional processes much more efficient than those common on the Earth. Because of the lower atmospheric temperature and the larger mean molecular weight of the Martian atmosphere the velocity of sound on Mars is less than on Earth. Velocities required to just initiate particle motion (Fig. 29), correspond to velocities of ~ 70 m/sec above the boundary layer, or Mach 0.4. Considerably higher velocities may be expected, at least at some places and times. Mars therefore presents an unusual possibility: that wind velocities in the transonic range (between Mach 0.9 and 1.0) occasionally exist. The erosional, depositional, and deflationary effects of transonic meteorology, if it exists, remain entirely unexplored.

Conclusions

We have found splotches and streaks as the albedo fine structure of Martian bright and dark areas. The superposition of splotches and streaks seems to determine the configuration of ground-based albedo markings. Both splotches and streaks vary on characteristic time scales of the order of 2 weeks. The integration of such variations is suggested to be the cause of the classical seasonal and secular variations, although no clear dependence of changes on latitude or season is found in these preliminary results. Aeolian transport of fine particles appears clearly to be implicated in the morphology and variation of splotches and streaks. We suggest that both bright and dark material is laterally transported on Mars.

Acknowledgments

We thank all those at the Jet Propulsion Laboratory whose collective efforts led to the success of this remarkable mission; and to our fellow members of the Mariner 9 television team who accommodated the variable surface features segment of the mission into the picture budget. John McCarthy, Director of the Artificial

Intelligence Laboratory (AIL) at Stanford University, was instrumental in making possible the calibration, registration, scaling, and picture differencing protocol used in the present paper. B. Eross, L. Wasserman, M. Noland, S. Saunders, and T. Kirby rendered specific assistance. We also thank William Green and the staff of the Image Processing Laboratory at JPL for picture processing. We are grateful to J. Cutts and C. Leovy for constructive reading of an earlier draft of this paper. This research was sponsored by NASA, through JPL. AIL was also supported by NASA grant NGR-05-020-508 and by ARPA grant SD-183.

References

ANTONIADI, E. M. (1930). "La Planète Mars." Hermann, Paris.

BAGNOLD, R. A., (1960). "The Physics of Blown Sand and Desert Dunes." Methuen, London.

BELCHER, D., VEVERKA, J., AND SAGAN, C. (1971). Mariner photography of Mars and aerial photography of Earth: Some analogies. *Icarus* **15**, 241–252.

DE VAUCOULEURS, G. (1954). "Physics of the Planet Mars." Faber and Faber, London.

DOLLFUS, A. (1968). Private communication.

FOCAS, J. H. (1961). Etude photometrique et polarimetrique des phenomene saisonniers de la planete Mars. *Ann. Astrophys.* **24**, 309–325.

FOCAS, J. H. (1962). Seasonal evolution of the fine structure of the dark areas of Mars *Planet. Space Sci.* **9**, 371–381.

GIERASCH, P., AND SAGAN, C. (1971). A preliminary assessment of Martian wind regimes. *Icarus* **14**, 312–318.

GIFFORD, F. A. (1964). The Martian canals according to a purely aeolian hypothesis. *Icarus* **3**, 130–135.

HANEL, R., CONRATH, B., HOVIS, W., KUNDE, V., LOWMAN, P., MACGUIRE, W., PEARL, J., PIRRAGLIA, J., PRABHAKARA, C., AND SCHLACHMAN, B. (1972). Investigation of the Martian environment by infrared spectroscopy on Mariner 9. *Icarus* **17**, 423–442.

HERTZLER, R. G. (1966a). Particle behavior in a simulated Martian environment. McDonnell Corporation Report E 418.

HERTZLER, R. G. (1966*b*). Behavior and characteristics of simulated Martian sand and dust storms. McDonnell Corporation Report E 720.

HORD, C. W., BARTH, C. A., STEWART, I. A., AND LANE, A. L. (1972). Mariner 9 ultraviolet spectrometer experiment: photometry and topography of Mars. *Icarus* **17**, 443–456.

LEOVY, C. B., BRIGGS, G. A., YOUNG, A. T., SMITH, B. A., POLLACK, J. B., SHIPLEY, E. N., AND WILDEY, R. L. (1972). Mariner 9 TV experiment: progress report on studies of Mars atmosphere. *Icarus* **17**, 373–393.

LEVINTHAL, E. C., GREEN, W. B., CUTTS, J. A., SANDER, M. J., SEIDMAN, J. B., YOUNG, A. T., AND SODERBLOM, L. A. (1973). Mariner 9—image processing and products. *Icarus* **18**, in press.

MASURSKY, H., BATSON, R., BORGESON, W., CARR, M., MCCAULEY, J., MILTON, D., WILDEY, R., WILHELMS, D., MURRAY, B., HOROWITZ, N., LEIGHTON, R., SHARP, R., THOMPSON, W., BRIGGS, G., CHANDEYSSON, P., SHIPLEY, E., SAGAN, C., POLLACK, J., LEDERBERG, J., LEVINTHAL, E., HARTMANN, W., MCCORD, T., SMITH, B., DAVIES, M., DE VAUCOULEURS, G., AND LEOVY, C. (1970). Television experiment for Mariner Mars 1971. *Icarus* **12**, 10–45.

MASURSKY, H., BATSON, R. M., MCCAULEY, J. F., SODERBLOM, L. A., WILDEY, R. L., CARR, M. H., MILTON, D. J., WILHELMS, D. E., SMITH, B. A., KIRBY, T. B., ROBINSON, J. C., LEOVY, C. B., BRIGGS, G. A., DUXBURY, T. C., ACTON, C. H., MURRAY, B. C., CUTTS, J. A., SHARP, R. P., SMITH, S., LEIGHTON, R. B., SAGAN, C., VEVERKA, J., NOLAND, M., DE VAUCOULEURS, G., DAVIES, M., AND YOUNG, A. T. (1972). Mariner 9 television reconnaissance of Mars and its satellites: Preliminary results. *Science* **175**, 294–304.

MCLAUGHLIN, D. B. (1955). Changes on Mars, as evidence of wind deposition and volcanism. *Astronom. J.* **60**, 261–270.

NEUGEBAUER, MUNCH G., KIEFFER, H., CHASE, S. C., JR., AND MINER, E. (1972). Mariner 1969 infrared radiometer results: temperatures and thermal properties of the Martian surface. *Astron. J.* in press.

POLLACK, J. B., GREENBERG, E., AND SAGAN, C. (1967). A statistical analysis of the Martian wave of darkening and related phenomena. *Planet. Space Sci.* **15**, 817–827.

SAGAN, C., AND POLLACK, J. B. (1967). A windblown dust model of Martian surface features and seasonal changes. Smithsonian Astrophysical Observatory Special Report 255.

SAGAN, C., AND POLLACK, J. B. (1969). Windblown dust on Mars. *Nature (London)* **223**, 791–794.

SAGAN, C., VEVERKA, J., AND GIERASCH, P. (1971). Observational consequences of Martian wind regimes. *Icarus* **15**, 253.

SLIPHER, E. C. (1962). Mars. Lowell Observatory. Flagstaff, Arizona.

Discussion

MAROV: You suggest that particle size differences are responsible for contrasting brightness of streaks and splotches. What differences in particle contrasts with color did you observe?

SAGAN: The three color filters carried on the A-Camera are not different enough in effective wavelength to provide much color information. Also, the filter wheel stuck in one filter position soon after the dust cleared making subsequent color measurements impossible.

MAROV: Are the particle size differences required to explain the contrasts of the streaks consistent with your earlier paper?

SAGAN: Yes. The size differences required is smaller than a factor of ten.

MAROV: The Mars 2 and 3 spacecrafts observed increasing in brightness contrasts of from about 10% at 0.7μm to about 20% at 1.4μm.

YOUNG: As a way of calibrating your eye when studying the Mariner Mars picture, the shadows of the two dust spots on the vidicon face plate have a contrast of 6% at all wavelengths.

MCCORD: The differences between the bright and dark regions cannot be explained by particle size differences alone. The spectral reflectivity differences and particularly the absorption band differences in the reflection spectra for bright and dark areas require that compositional differences exist, such as differences in the amount of oxidized basalt as John Adams and I have suggested. Particle size differences may also occur, of course.

SAGAN: Yes. Real compositional differences are possible, and we have suggested that chemical composition and particle size are correlated (C. Sagan, J. Veverka, P. Gierasch. *Icarus* **15**, 253, 1971).

MCCORD: There is, in fact, a photo-oxidation mechanism which a graduate student of mine, Bob Huguenin, has discovered which explains nicely how the surface of Mars could have been oxidized to produce contrasting bright and dark material of different degrees of oxidation. It also turns out that the more oxidized material is more easily broken into small grains.

IRVINE: Are there any bright dune fields? Could the darkness of dune fields be due to a shadow effect?

SAGAN: No. The brightest part of the dune fields are darker than the surrounding areas.

HARTMANN: The classical dark areas do seem to have dark background material in addition to the dark streaks. Is this what you see also?

SAGAN: Yes. The dark background may be left over from previous tails.

RUNCORN: What is the scale of the dune fields? The entire field and one dune to another?

SAGAN: About 50km across the field and about 2km crest-to-crest for the dunes.